Extending SkyLLH software for neutrino point source analyses with 10 years of IceCube public data

The IceCube Collaboration

(a complete list of authors can be found at the end of the proceedings)

E-mail: chiara.bellenghi@tum.de, martina.karl@tum.de, martin.wolf@tum.de

Searching for the sources of high-energy cosmic particles requires sophisticated analysis techniques, frequently involving hypothesis tests with unbinned log-likelihood (LLH) functions. SkyLLH is an open-source, Python-based software tool to build these LLH functions and perform likelihood-ratio tests. We present a new easy-to-use and modular extension of SkyLLH that allows the user to perform neutrino point source searches in the entire sky using ten years of IceCube public data. To guide the user, SkyLLH provides tutorials showing how to analyze the experimental data and calculate useful statistical quantities. Here we describe the details of the analysis workflow and illustrate some of the possible methods to work with the IceCube public dataset. Additionally, we show that SkyLLH can reproduce the results from a previous IceCube publication that used the public data release. We obtain a similar local significance for the neutrino emission from a list of candidate sources within a maximum shift of 0.5σ. Finally, the measured neutrino flux from the most significant source candidate, NGC 1068, shows substantial agreement with the previously published result.

Corresponding authors: Chiara Bellenghi[1][*], Martina Karl[1,2], Martin Wolf[1]

[1] *Technical University of Munich, TUM School of Natural Sciences, Department of Physics, James-Franck-Straße 1, D-85748 Garching bei München, Germany*
[2] *European Southern Observatory, Karl-Schwarzschild-Straße 2, D-85748 Garching bei München, Germany*

[*] Presenter

1. Introduction

SkyLLH [1] is an open-source, Python-based, and easy-to-use software framework to build log-likelihood (LLH) functions for celestial event data. It has been developed within the IceCube collaboration [2] to perform frequentist statistical data analyses for point-like neutrino source searches, including the one that resulted in a $4.2\,\sigma$ evidence for neutrino emission from the Seyfert II galaxy NGC 1068 [3]. In the past, IceCube performed searches for steady and flaring neutrino point-like sources using 10 years of point-source data [4, 5]. This data has been made public [6]. In order to make this information accessible and usable for the entire community, we present an extension to the SkyLLH software framework which now includes an interface to use this latest all-sky point-source data release. In the following, we briefly describe the content of the data release and detail the likelihood method that has been implemented for point-like neutrino searches. The published experimental data are provided together with binned detector response functions that describe how a muon produced in the interaction of a detectable neutrino would be reconstructed in IceCube. Among the reconstructed muon observables given in the detector response functions is the angular separation between the parent neutrino and the reconstructed muon. This quantity is fundamental for inferring whether the spatial distribution of the events in the sky is consistent with emission from a point-like source. On the other hand, the reconstructed muon direction is also required in the formulation of the likelihood function used in Ref. [4] but is not provided in the detector response functions. Nevertheless, we can address this limitation by using a slightly modified version of the likelihood. We investigate the effect of this modification by comparing the likelihoods of the internal and the public analyses. Furthermore, we fit the source candidates that were searched for neutrino emission in Ref. [4] and compare their significance to the published one. For NGC 1068 specifically, we measure the neutrino flux and compare the result to the one reported in Ref. [4]. Finally, we briefly describe a method to fit time-dependent neutrino emission profiles from point-like sources, which is implemented in the software interface for public neutrino data analyses described in this work.

2. The 10 years of public neutrino point-source data

In January 2021, IceCube released ten years of data for neutrino point-source searches [6]. The data spans the time range from April 6, 2008 to July 10, 2018, covering five different data acquisition periods (seasons) corresponding to different detector configurations: IC40, IC59, IC79, IC86 2011, and IC86 2012–2017. For details regarding the IceCube detector see Ref. [2]. The data sample is optimized for the identification of neutrino clusters, which requires good angular resolution. Therefore, it includes track-like events from all directions in the sky. In the Southern sky, the data sample is dominated by cosmic-ray-induced atmospheric muons, which are instead absorbed in the other hemisphere when crossing the Earth. Therefore, events from the Northern sky are mostly produced in neutrino interactions. The data contains 1,134,450 recorded events with their best-fit reconstructed muon observables $\vec{x} = (E_\mu, \vec{d}_\mu, \sigma_\mu, t_{\text{obs}})$: the energy E_μ, direction in right-ascension α and declination δ, $\vec{d}_\mu = (\alpha_\mu, \delta_\mu)$, the uncertainty on the reconstructed muon direction σ_μ, as well as the observation time t_{obs}. It should be noted that the angular uncertainty includes a correction for the kinematic angle between the parent neutrino and the reconstructed muon, important for

neutrino energies $\lesssim 1$ TeV. In addition, the release provides tabulated instrument response functions (IRFs) consisting of muon-neutrino effective areas, $A_{\text{eff},\nu_\mu+\bar{\nu}_\mu}$, and binned probabilities in the form $M(E_\mu, \Psi_{\nu\mu}, \sigma_\mu|\delta_\nu, E_\nu)$. Thus, for a given parent neutrino with declination δ_ν and energy E_ν, M contains the probability of reconstructing a neutrino-induced muon with E_μ, σ_μ, and an angular separation $\Psi_{\nu\mu}$ between the parent neutrino and the muon. M is referred to as the detector response matrix from here on[1]. The published IRFs allow the construction of the probability density functions (PDFs) required in a hypothesis log-likelihood ratio test.

3. Likelihood formalism

The IceCube point-source searches look for spatial and/or temporal clusters of astrophysical neutrinos over the atmospheric muon and neutrino, and diffuse cosmic neutrino backgrounds [7]. To be able to discriminate between signal and background events, IceCube uses an unbinned likelihood-ratio hypothesis test, where two hypotheses are fitted to the data, and their likelihoods are compared:

- H_0: the observed data only consists of background muon events, induced by atmospheric muons and neutrinos or by the astrophysical diffuse neutrino flux;

- H_1: the observed data consists of, both, background and signal muon events, where the latter are induced by the interaction of astrophysical neutrinos originating from a point-like neutrino source, emitting with strength proportional to the mean number of signal events in the detector, n_s, and following a power-law energy spectrum $\propto E^{-\gamma}$.

The two hypotheses are nested. Hence, for $n_s \equiv 0$, the signal hypothesis, H_1, reduces to the background-only one, H_0. The maximum log-likelihood ratio is then the test-statistic, TS, used for the analysis:

$$\text{TS} = -2 \log \frac{\sup_{H_0} [\mathcal{L}(H_0|\vec{x})]}{\sup_{H_1} [\mathcal{L}(H_1|\vec{x})]}, \tag{1}$$

where $\mathcal{L}(H|\vec{x})$ is the likelihood function of H_0 or H_1, given the recorded data $\vec{x}$. The likelihood function is commonly represented as a mixture model, consisting of the weighted sum of a signal PDF and a background PDF, $\mathcal{S}(\cdot)$ and $\mathcal{B}(\cdot)$, respectively [8]:

$$\mathcal{L}(n_s, \gamma|\vec{x}) = \prod_{i=1}^{N} \left[\frac{n_s}{N} \mathcal{S}(x_i|\gamma) + \left(1 - \frac{n_s}{N}\right) \mathcal{B}(x_i) \right], \tag{2}$$

where N is the total number of events x_i in the sample.

For the nested hypotheses used in point-source searches as described here, the null hypothesis H_0 has no free parameters, hence the test-statistic can be written as a simplified expression containing the signal-over-background PDF ratio:

$$\text{TS} = 2 \sum_{i=1}^{N} \log \left[\frac{\hat{n}_s}{N} \left(\frac{\mathcal{S}(x_i|\hat{\gamma})}{\mathcal{B}(x_i)} - 1 \right) + 1 \right]. \tag{3}$$

Here the parameters $\hat{n}_s$ and $\hat{\gamma}$ denote the values of the two parameters that maximize the likelihood in Eq. (2).

---

[1]It is denoted as *smearing matrix* in the data release [6].

The new extension of SkyLLH for the public data provides classes and functions to construct the signal and background PDFs using the provided experimental data and IRFs. By using the law of conditional probability, both the signal and background PDFs can be separated into a spatial and an energy part. Spatial and energy background PDFs are defined identically to the internal traditional IceCube analysis (see *e.g.* Ref. [4]), therefore we assume that the background flux is uniformly distributed in space and that its energy distribution can be approximated by the energy distribution of the experimental data. This assumes that the experimental data is strongly dominated by background events, which is a safe assumption in this case.

The signal PDF for a point-like source with a power-law energy spectrum is dependent on the source declination δ_{src}[2] and the spectral index γ and can be expressed as

$$\mathcal{S}(\delta_i, E_i | \delta_{\mathrm{src}}, \gamma) = \mathcal{S}_{\mathrm{spatial}} \cdot \mathcal{S}_{\mathrm{energy}} = P_{\mathrm{PSF}}(\delta_i | \delta_{\mathrm{src}}) \cdot P_{\mathrm{E}}(E_i | \delta_{\mathrm{src}}, \gamma), \tag{4}$$

where P_{PSF} is the point-spread-function (PSF) of the detector for a given source position and $P_{\mathrm{E}}(E_i | \delta_{\mathrm{src}}, \gamma)$ is the signal energy PDF to observe an event with energy E_i assuming point-like neutrino emission from δ_{src} and spectral index γ. For the PSF an analytical function in the form of a symmetric two-dimensional Gaussian is used (*e.g.* Ref. [8], and Ref. [4]).

The signal energy PDF can be constructed from the detector response matrix M and can be formulated as an integral over all parent neutrino energies:

$$P_{\mathrm{E}}(E_i | \delta_{\mathrm{src}}, \gamma) \equiv P(E_\mu | \delta_\nu, \gamma) = \int_{E_{\mathrm{min}}}^{E_{\mathrm{max}}} dE_\nu \, P(E_\mu | E_\nu, \delta_\nu) \, P(E_\nu | \gamma) \, P(E_\nu | \delta_\nu). \tag{5}$$

The integrand is the product of three probabilities. First, $P(E_\mu | E_\nu, \delta_\nu)$ is the probability of E_μ given the parent neutrino energy E_ν and declination δ_ν, which is calculated from the detector response matrix M. Second, the probability of the parent neutrino energy for the given power-law energy spectrum with spectral index γ, denoted as $P(E_\nu | \gamma)$. Third, the probability of detecting the parent neutrino energy given its direction, $P(E_\nu | \delta_\nu)$, is calculated from the provided tabulated effective areas. The integration limits E_{min} and E_{max} are set in order to cover the parent neutrino energy range of $10^2 - 10^9$ GeV, as provided in the IRFs.

Only the mathematical representation of the signal energy PDF differs from the internal analysis used in Ref. [4]. Internally, it is constructed as $P(E_\mu | \sin(\delta_\mu), \gamma)$, whereas the public data analysis uses the signal energy PDF given in Eq. (5). The difference is illustrated in Figure 1 for the dataset IC86 2012–2017 and for a source at the location of NGC 1068 with its best-fit spectral index $\gamma = 3.2$ [3, 4]. The internal analysis uses the approximation $\delta_{\mathrm{src}} \approx \delta_\mu$ to simplify the calculation of the signal-over-background PDF ratio (see Eq. (3)), which then has the same data structure as the signal and background PDFs. With the public detector response matrix, the construction of such a signal energy PDF is impractical due to missing information about the reconstructed muon declination δ_μ.

4. Analysis workflow with SkyLLH

The SkyLLH software framework is designed to follow the mathematical structure of the log-likelihood ratio formalism in Eq. (3). Hence, Python base classes define interfaces for PDFs, PDF

---

[2]Due to the location of IceCube at the geographic South Pole, the distributions of the recorded events are symmetric in azimuth and hence depend in good approximation solely on the declination of the event.
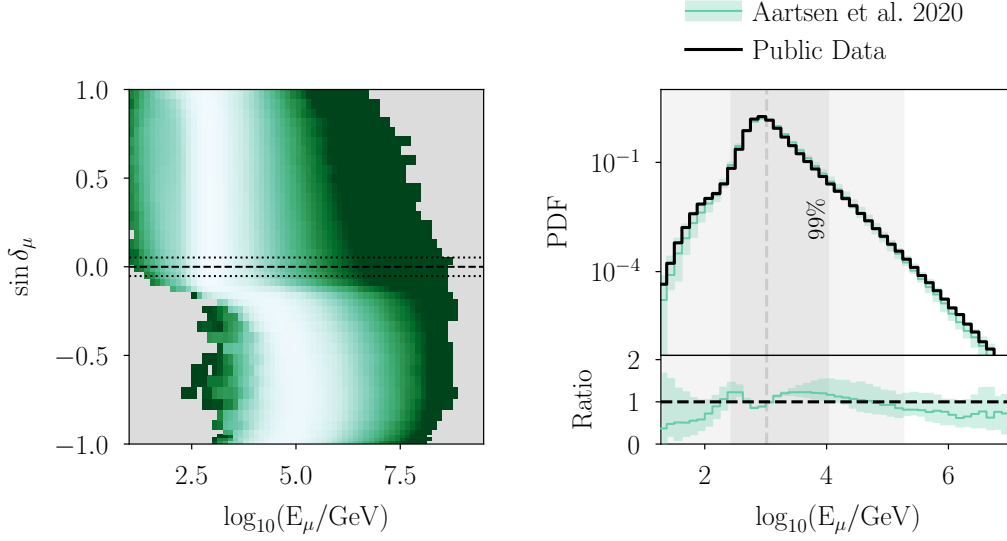
Figure 1: Comparison of the signal energy PDFs for the season IC86 2012–2017 and spectral index $\gamma = 3.2$. **Left**: PDF as used in Ref. [4]. The lighter the color, the higher the probability density. The black lines delimit $\delta_\mu = (-0.01 \pm 3.00)°$. **Right**: 1D comparison between the internal IceCube PDF (green) at reconstructed muon declination $\delta_\mu = -0.01°$ and the one used in the public data analysis (black) at source declination $\delta_{\rm src} = -0.01°$ (NGC 1068). The shaded green band represents the variations of the internal energy PDF when considering events reconstructed at declinations enclosed by the dotted black lines in the left-hand plot. The energies of the experimental data fall in the gray shaded area, with the central 99% quantile indicated by the darker grey area. The lower panel shows the ratio between the public PDF and the internal one for all events reconstructed within 3° from the source.

ratios, log-likelihood ratio, and test-statistic functions. The `Analysis` class bundles all components of an analysis into a single object. Despite classes and functions to evaluate the log-likelihood function, SkyLLH also provides utility classes for data handling. For instance, the `Dataset` class allows the definition of a data set with observed data and simulations stored on disk, and its loading into memory. The public data interface described in this contribution creates the `Analysis` object through a `create_analysis` Python function, which constructs all the necessary PDFs and PDF ratios, as well as the log-likelihood function. After the construction of the `Analysis` object, the data can either be unblinded via the `unblind` method or a pseudo-experiment with background and signal events can be generated via the `do_trial` method of the `Analysis` class. The documentation[3] of SkyLLH provides a tutorial to load the public data and to create the `Analysis` object for a single point-source with a power-law energy flux function to reproduce the results published in Ref. [4]. Furthermore, it shows how to generate pseudo-experiments for sensitivity and significance calculations. Notably, SkyLLH's design allows for a combined data analysis of multiple data sets or detectors by taking the product of all likelihood functions, one for each individual data set. Thus, the public data could be combined with data from other experiments.

---

[3] https://icecube.github.io/skyllh/master/html/index.html

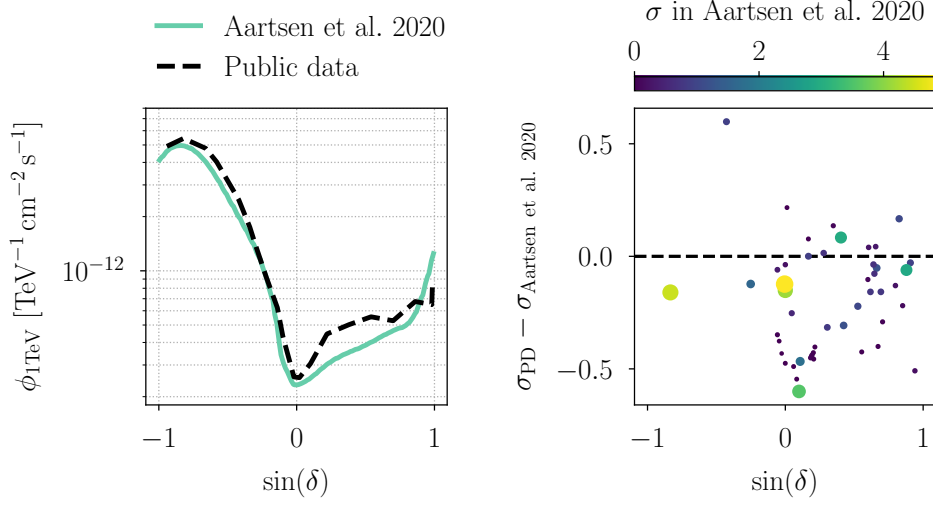## 5. Reproducibility of published IceCube point-source search results

To test how well the analysis published in Ref. [4] can be reproduced using the public data release and the software interface described in this contribution, we compare their respective sensitivities to an E^{-2} flux of astrophysical neutrinos produced by a point-like source. The result of this comparison is illustrated in the left panel of Figure 2 where the sensitivity flux is shown as a function of the sine of the declination for the public data (black dashed) and the internal IceCube analysis (green) as published in Ref. [4]. In the right panel of Figure 2, the local significance difference in terms of Gaussian-equivalent standard deviations for the source candidates analyzed in Ref. [4] is plotted as a function of their position in the sky. For most of the tested sources, the significance is weaker when using the public data (PD), but it is reproduced within ~ 0.5 standard deviations. Overall, the public data analysis is slightly less sensitive due to the coarse binning of the detector response matrix, which contains only 3 bins for the parent neutrino direction, covering the Southern sky ($-90° < \delta_\nu < -10°$), the horizon ($-10° < \delta_\nu < 10°$), and the Northern sky ($10° < \delta_\nu < 90°$). We measured the neutrino flux $\phi(E_\nu) = \phi_{1\text{TeV}} (E_\nu/1\text{TeV})^{-\gamma}$ from NGC 1068 with the public data analysis presented in this work and find the best-fit values for the flux parameters to be $\hat{n}_s = 60.1$, and $\hat{\gamma} = 3.2$. The observed mean number of signal events $\hat{n}_s$ can be converted into a neutrino flux normalization by integrating the effective area at the source location multiplied by the power-law energy flux over the neutrino energy range and the observation time period. We obtain $\hat{\phi}_{1\text{TeV}} = 3.3 \times 10^{-11} \text{ TeV}^{-1} \text{cm}^{-2} \text{s}^{-1}$. All these values are compatible with the ones published in Ref. [4]. As an additional check, we performed a likelihood scan around the best-fit flux parameters and derived the 1σ and 2σ confidence levels from Wilks' theorem [9]. The comparison of the likelihood landscapes is illustrated in Figure 3 showing that the two results largely overlap.

## 6. Sources with time-dependent neutrino emission profiles

The results shown in this contribution assume steady neutrino emission as done in Ref. [4]. Besides classes for spatial and energy PDFs, SkyLLH also provides a class for time PDFs. Hence, the signal PDF in Eq. (4) can be modified to include a time PDF:

$$\mathcal{S}(\delta_i, E_i | \delta_{\text{src}}, \gamma) = P_{\text{PSF}}(\delta_i | \delta_{\text{src}}) \cdot P_{\text{E}}(E_i | \delta_{\text{src}}, \gamma) \cdot P_{\text{T}}(t_i | t_0, \sigma_{\text{T}}). \quad (6)$$

The current version includes a box-shaped time PDF (assuming constant emission between a starting and end time) and a Gaussian-shaped time PDF centered at t_0 with width σ_{T}. Using the box-shaped time profile from Ref. [6] with start and stop times, respectively, of $t_{\text{start}} = 56927.86$ (MJD) and $t_{\text{stop}} = 57116.76$ (MJD), the best-fit parameters for the flare of the blazar TXS 0506+056 are $\hat{n}_s = 11.66$ and $\hat{\gamma} = 2.25$, agree with values published in Ref. [6], namely $\hat{n}_s = 11.87$ and $\hat{\gamma} = 2.22$. SkyLLH supports the fitting of the parameters of a Gaussian-shaped time PDF (i.e., t_0, σ_{T}) using the unsupervised learning algorithm "Expectation Maximization (EM)" [10]. EM is applied to the time sequence of the events, where each event is weighted with its signal-over-background PDF ratio of the spatial and energy PDFs, as in Eq. (3). With the fitted parameters, we create the time PDF and subsequently optimize the likelihood function. Since the PDF ratio values depend on γ, we repeat these steps for γ values ranging from 1 to 5 and take the maximal test-statistic from all EM fits as the final test-statistic value. The EM method was used in Ref. [11] with IceCube internal

Figure 2: Reproducibility of published results. **Left:** Comparison of sensitivity to an astrophysical neutrino flux as a function of the position in the sky assuming an E^{-2} power-law energy spectrum for the analysis used in Ref. [4] (green solid line) and the public data (PD) analysis presented in this work (dashed black line). **Right:** Shift of local significance in terms of Gaussian-equivalent standard deviations as a function of the sine of the declination compared to the result published in Ref. [4]. The dots represent the objects in the list of candidate sources in Ref. [4] and the two most significant locations in the northern and southern sky. The color scale, as well as the size of the dots, represent the published local significance. The green point with the largest shift to lower significances (at the very bottom of the panel) corresponds to TXS 0506+056.
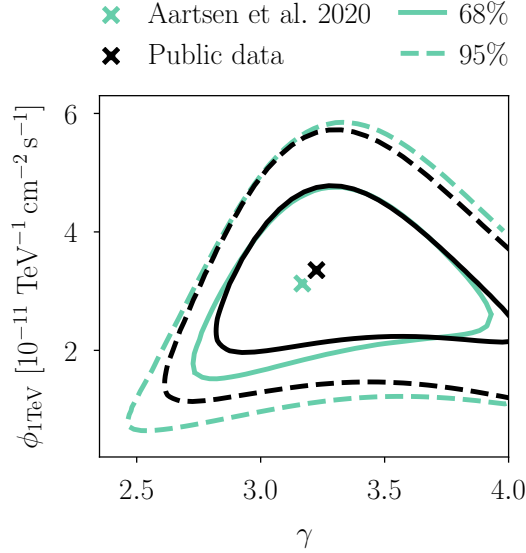
Figure 3: Comparison of the likelihood scan around the best-fit flux parameters ($\phi_{1\text{TeV}}$, γ) of NGC 1068. The best-fit flux (cross), 1σ (solid line), and 2σ (dashed line) confidence levels from Wilks' theorem are shown in green for the analysis in Ref. [4] and in black for the analysis on public data presented in this work.

data where the fitted flare parameter and the p-value for the flare of TXS 0506+056 are comparable with published results in Ref. [5, 6, 12]. With the published data set we estimate the significance of the observed flare (using EM) and find a local p-value of $-\log_{10}(p_{\text{loc}}) = 1.23$. The reduced p-value compared to previous works is expected, see also Section 5, Figure 2. The best-fit parameters for the time-dependent neutrino emission from TXS 0506+056 using the public data are $\hat{n}_s = 7.58$ and $\hat{\gamma} = 2.21$, centered at $\hat{t}_0 = 56972.65$ (MJD) with $\hat{\sigma}_T = 27.97$ days. In Ref. [5], the flare parameters were $\hat{t}_0 = 57000 \pm 30$ (MJD), $\hat{\sigma}_T = 62 \pm 27$ days, $\hat{n}_s = 10^{+5.2}_{-4.2}$, and $\hat{\gamma} = 2.2 \pm 0.3$. However, it should be noted that the fitting and analysis procedures in Ref. [5] are different, specifically concerning the signal energy PDF (see Section 3) and, therefore, the signal-over-background PDF-ratio weights.

7. Conclusion and outlook

In this contribution, we demonstrated an extension of SkyLLH to perform time-integrated and time-dependent neutrino point-source searches based on 10-year public point-source data. By using this extension, published IceCube results [4] can be reproduced reasonably well. We plan to implement additional features to support general source flux functions and the ability to evaluate the cumulated signal from multiple sources through point-source stacking analyses in the future.

References

[1] **IceCube** Collaboration, T. Kontrimas, M. Wolf, *et al. PoS* **ICRC2021** (2022) 1073.

[2] **IceCube** Collaboration, M. G. Aartsen *et al. JINST* **12** no. 03, (2017) P03012.

[3] **IceCube** Collaboration, R. Abbasi *et al. Science* **378** no. 6619, (2022) 538–543.

[4] **IceCube** Collaboration, M. G. Aartsen *et al. Phys. Rev. Lett.* **124** (Feb, 2020) 051103.

[5] **IceCube** Collaboration, R. Abbasi *et al. The Astrophysical Journal Letters* **920** no. 2, (Oct, 2021) L45.

[6] **IceCube** Collaboration, R. Abbasi *et al.*, "IceCube Data for Neutrino Point-Source Searches Years 2008-2018," 2021. https://arxiv.org/abs/2101.09836.

[7] **IceCube** Collaboration, R. Abbasi *et al. The Astrophysical Journal Letters* **928** no. 1, (Mar., 2022) 50.

[8] J. Braun *et al. Astroparticle Physics* **29** no. 4, (2008) 299–305.

[9] S. S. Wilks *The Annals of Mathematical Statistics* **9** no. 1, (1938) 60–62.

[10] A. P. Dempster *et al. Journal of the Royal Statistical Society. Series B (Methodological)* **39** no. 1, (1977) 1–38.

[11] **IceCube** Collaboration, M. Karl *PoS* **ICRC2023** (these proceedings) 974.

[12] **IceCube** Collaboration, M. Aartsen *et al. Science* **361** no. 6398, (2018) 147–151.

Full Author List: IceCube Collaboration

R. Abbasi[17], M. Ackermann[63], J. Adams[18], S. K. Agarwalla[40, 64], J. A. Aguilar[12], M. Ahlers[22], J.M. Alameddine[23], N. M. Amin[44], K. Andeen[42], G. Anton[26], C. Argüelles[14], Y. Ashida[53], S. Athanasiadou[63], S. N. Axani[44], X. Bai[50], A. Balagopal V.[40], M. Baricevic[40], S. W. Barwick[30], V. Basu[40], R. Bay[8], J. J. Beatty[20, 21], J. Becker Tjus[11, 65], J. Beise[61], C. Bellenghi[27], C. Benning[1], S. BenZvi[52], D. Berley[19], E. Bernardini[48], D. Z. Besson[36], E. Blaufuss[19], S. Blot[63], F. Bontempo[31], J. Y. Book[14], C. Boscolo Meneguolo[48], S. Böser[41], O. Botner[61], J. Böttcher[1], E. Bourbeau[22], J. Braun[40], B. Brinson[6], J. Brostean-Kaiser[63], R. T. Burley[2], R. S. Busse[43], D. Butterfield[40], M. A. Campana[49], K. Carloni[14], E. G. Carnie-Bronca[2], S. Chattopadhyay[40, 64], N. Chau[12], C. Chen[6], Z. Chen[55], D. Chirkin[40], S. Choi[56], B. A. Clark[19], L. Classen[43], A. Coleman[61], G. H. Collin[15], A. Connolly[20, 21], J. M. Conrad[15], P. Coppin[13], P. Correa[13], D. F. Cowen[59, 60], P. Dave[6], C. De Clercq[13], J. J. DeLaunay[58], D. Delgado[14], S. Deng[1], K. Deoskar[54], A. Desai[40], P. Desiati[40], K. D. de Vries[13], G. de Wasseige[37], T. DeYoung[24], A. Diaz[15], J. C. Díaz-Vélez[40], M. Dittmer[43], A. Domi[26], H. Dujmovic[40], M. A. DuVernois[40], T. Ehrhardt[41], P. Eller[27], E. Ellinger[62], S. El Mentawi[1], D. Elsässer[23], R. Engel[31, 32], H. Erpenbeck[40], J. Evans[19], P. A. Evenson[44], K. L. Fan[19], K. Fang[40], K. Farrag[16], A. R. Fazely[7], A. Fedynitch[57], N. Feigl[10], S. Fiedlschuster[26], C. Finley[54], L. Fischer[63], D. Fox[59], A. Franckowiak[11], A. Fritz[41], P. Fürst[1], J. Gallagher[39], E. Ganster[1], A. Garcia[14], L. Gerhardt[9], A. Ghadimi[58], C. Glaser[61], T. Glauch[27], T. Glüsenkamp[26, 61], N. Goehlke[32], J. G. Gonzalez[44], S. Goswami[58], D. Grant[24], S. J. Gray[19], O. Gries[1], S. Griffin[40], S. Griswold[52], K. M. Groth[22], C. Günther[1], P. Gutjahr[23], C. Haack[26], A. Hallgren[61], R. Halliday[24], L. Halve[1], F. Halzen[40], H. Hamdaoui[55], M. Ha Minh[27], K. Hanson[40], J. Hardin[15], A. A. Harnisch[24], P. Hatch[33], A. Haungs[31], K. Helbing[62], J. Hellrung[11], F. Henningsen[27], L. Heuermann[1], N. Heyer[61], S. Hickford[62], A. Hidvegi[54], C. Hill[16], G. C. Hill[2], K. D. Hoffman[19], S. Hori[40], K. Hoshina[40, 66], W. Hou[31], T. Huber[31], K. Hultqvist[54], M. Hünnefeld[23], R. Hussain[40], K. Hymon[23], S. In[56], A. Ishihara[16], M. Jacquart[40], O. Janik[1], M. Jansson[54], G. S. Japaridze[5], M. Jeong[56], M. Jin[14], B. J. P. Jones[4], D. Kang[31], W. Kang[56], X. Kang[49], A. Kappes[43], D. Kappesser[41], L. Kardum[23], T. Karg[63], M. Karl[27], A. Karle[40], U. Katz[26], M. Kauer[40], J. L. Kelley[40], A. Khatee Zathul[40], A. Kheirandish[34, 35], J. Kiryluk[55], S. R. Klein[8, 9], A. Kochocki[24], R. Koirala[44], H. Kolanoski[10], T. Kontrimas[27], L. Köpke[41], C. Kopper[26], D. J. Koskinen[22], P. Koundal[31], M. Kovacevich[49], M. Kowalski[10, 63], T. Kozynets[22], J. Krishnamoorthi[40, 64], K. Kruiswijk[37], E. Krupczak[24], A. Kumar[63], E. Kun[11], N. Kurahashi[49], N. Lad[63], C. Lagunas Gualda[63], M. Lamoureux[37], M. J. Larson[19], S. Latseva[1], F. Lauber[62], J. P. Lazar[14, 40], J. W. Lee[56], K. Leonard DeHolton[60], A. Leszczyńska[44], M. Lincetto[11], Q. R. Liu[40], M. Liubarska[25], E. Lohfink[41], C. Love[49], C. J. Lozano Mariscal[43], L. Lu[40], F. Lucarelli[28], W. Luszczak[20, 21], Y. Lyu[8, 9], J. Madsen[40], K. B. M. Mahn[24], Y. Makino[40], E. Manao[27], S. Mancina[40, 48], W. Marie Sainte[40], I. C. Mariş[12], S. Marka[46], Z. Marka[46], M. Marsee[58], I. Martinez-Soler[14], R. Maruyama[45], F. Mayhew[24], T. McElroy[25], F. McNally[38], J. V. Mead[22], K. Meagher[40], S. Mechbal[63], A. Medina[21], M. Meier[16], Y. Merckx[13], L. Merten[11], J. Micallef[24], J. Mitchell[7], T. Montaruli[28], R. W. Moore[25], Y. Morii[16], R. Morse[40], M. Moulai[40], T. Mukherjee[31], R. Naab[63], R. Nagai[16], M. Nakos[40], U. Naumann[62], J. Necker[63], A. Negi[4], M. Neumann[43], H. Niederhausen[24], M. U. Nisa[24], A. Noell[1], A. Novikov[44], S. C. Nowicki[24], A. Obertacke Pollmann[16], V. O'Dell[40], M. Oehler[31], B. Oeyen[29], A. Olivas[19], R. Ørsøe[27], J. Osborn[40], E. O'Sullivan[61], H. Pandya[44], N. Park[33], G. K. Parker[4], E. N. Paudel[44], L. Paul[42, 50], C. Pérez de los Heros[61], J. Peterson[40], S. Philippen[1], A. Pizzuto[40], M. Plum[50], A. Pontén[61], Y. Popovych[41], M. Prado Rodriguez[40], B. Pries[24], R. Procter-Murphy[19], G. T. Przybylski[9], C. Raab[37], J. Rack-Helleis[41], K. Rawlins[3], Z. Rechav[40], A. Rehman[44], P. Reichherzer[11], G. Renzi[12], E. Resconi[27], S. Reusch[63], W. Rhode[23], B. Riedel[40], A. Rifaie[1], E. J. Roberts[2], S. Robertson[8, 9], S. Rodan[56], G. Roellinghoff[56], M. Rongen[26], C. Rott[53, 56], T. Ruhe[23], L. Ruohan[27], D. Ryckbosch[29], I. Safa[14, 40], J. Saffer[32], D. Salazar-Gallegos[24], P. Sampathkumar[31], S. E. Sanchez Herrera[24], A. Sandrock[62], M. Santander[58], S. Sarkar[25], S. Sarkar[47], J. Savelberg[1], P. Savina[40], M. Schaufel[1], H. Schieler[31], S. Schindler[26], L. Schlickmann[1], B. Schlüter[43], F. Schlüter[12], N. Schmeisser[62], T. Schmidt[19], J. Schneider[26], F. G. Schröder[31, 44], L. Schumacher[26], G. Schwefer[1], S. Sclafani[19], D. Seckel[44], M. Seikh[36], S. Seunarine[51], R. Shah[49], A. Sharma[61], S. Shefali[32], N. Shimizu[16], M. Silva[40], B. Skrzypek[14], B. Smithers[4], R. Snihur[40], J. Soedingrekso[23], A. Søgaard[22], D. Soldin[32], P. Soldin[1], G. Sommani[11], C. Spannfellner[27], G. M. Spiczak[51], C. Spiering[63], M. Stamatikos[21], T. Stanev[44], T. Stezelberger[9], T. Stürwald[62], T. Stuttard[22], G. W. Sullivan[19], I. Taboada[6], S. Ter-Antonyan[7], M. Thiesmeyer[1], W. G. Thompson[14], J. Thwaites[40], S. Tilav[44], K. Tollefson[24], C. Tönnis[56], S. Toscano[12], D. Tosi[40], A. Trettin[63], C. F. Tung[6], R. Turcotte[31], J. P. Twagirayezu[24], B. Ty[40], M. A. Unland Elorrieta[43], A. K. Upadhyay[40, 64], K. Upshaw[7], N. Valtonen-Mattila[61], J. Vandenbroucke[40], N. van Eijndhoven[13], D. Vannerom[15], J. van Santen[63], J. Vara[43], J. Veitch-Michaelis[40], M. Venugopal[31], M. Vereecken[37], S. Verpoest[44], D. Veske[46], A. Vijai[19], C. Walck[54], C. Weaver[24], P. Weigel[15], A. Weindl[31], J. Weldert[60], C. Wendt[40], J. Werthebach[23], M. Weyrauch[31], N. Whitehorn[24], C. H. Wiebusch[1], N. Willey[24], D. R. Williams[58], L. Witthaus[23], A. Wolf[1], M. Wolf[27], G. Wrede[26], X. W. Xu[7], J. P. Yanez[25], E. Yildizci[40], S. Yoshida[16], R. Young[36], F. Yu[14], S. Yu[24], T. Yuan[40], Z. Zhang[55], P. Zhelnin[14], M. Zimmerman[40]

[1] III. Physikalisches Institut, RWTH Aachen University, D-52056 Aachen, Germany

[2] Department of Physics, University of Adelaide, Adelaide, 5005, Australia

[3] Dept. of Physics and Astronomy, University of Alaska Anchorage, 3211 Providence Dr., Anchorage, AK 99508, USA

[4] Dept. of Physics, University of Texas at Arlington, 502 Yates St., Science Hall Rm 108, Box 19059, Arlington, TX 76019, USA

[5] CTSPS, Clark-Atlanta University, Atlanta, GA 30314, USA

[6] School of Physics and Center for Relativistic Astrophysics, Georgia Institute of Technology, Atlanta, GA 30332, USA

[7] Dept. of Physics, Southern University, Baton Rouge, LA 70813, USA

[8] Dept. of Physics, University of California, Berkeley, CA 94720, USA

[9] Lawrence Berkeley National Laboratory, Berkeley, CA 94720, USA

[10] Institut für Physik, Humboldt-Universität zu Berlin, D-12489 Berlin, Germany

[11] Fakultät für Physik & Astronomie, Ruhr-Universität Bochum, D-44780 Bochum, Germany

[12] Université Libre de Bruxelles, Science Faculty CP230, B-1050 Brussels, Belgium

[13] Vrije Universiteit Brussel (VUB), Dienst ELEM, B-1050 Brussels, Belgium

[14] Department of Physics and Laboratory for Particle Physics and Cosmology, Harvard University, Cambridge, MA 02138, USA

[15] Dept. of Physics, Massachusetts Institute of Technology, Cambridge, MA 02139, USA

[16] Dept. of Physics and The International Center for Hadron Astrophysics, Chiba University, Chiba 263-8522, Japan

[17] Department of Physics, Loyola University Chicago, Chicago, IL 60660, USA

[18] Dept. of Physics, University of Canterbury, Private Bag 4800, Christchurch, New Zealand

[19] Dept. of Physics, University of Maryland, College Park, MD 20742, USA

[20] Dept. of Astronomy, Ohio State University, Columbus, OH 43210, USA

[21] Dept. of Physics and Center for Cosmology and Astro-Particle Physics, Ohio State University, Columbus, OH 43210, USA

[22] Niels Bohr Institute, University of Copenhagen, DK-2100 Copenhagen, Denmark

[23] Dept. of Physics, TU Dortmund University, D-44221 Dortmund, Germany

[24] Dept. of Physics and Astronomy, Michigan State University, East Lansing, MI 48824, USA

[25] Dept. of Physics, University of Alberta, Edmonton, Alberta, Canada T6G 2E1

[26] Erlangen Centre for Astroparticle Physics, Friedrich-Alexander-Universität Erlangen-Nürnberg, D-91058 Erlangen, Germany

[27] Technical University of Munich, TUM School of Natural Sciences, Department of Physics, D-85748 Garching bei München, Germany

[28] Département de physique nucléaire et corpusculaire, Université de Genève, CH-1211 Genève, Switzerland

[29] Dept. of Physics and Astronomy, University of Gent, B-9000 Gent, Belgium

[30] Dept. of Physics and Astronomy, University of California, Irvine, CA 92697, USA

[31] Karlsruhe Institute of Technology, Institute for Astroparticle Physics, D-76021 Karlsruhe, Germany

[32] Karlsruhe Institute of Technology, Institute of Experimental Particle Physics, D-76021 Karlsruhe, Germany

[33] Dept. of Physics, Engineering Physics, and Astronomy, Queen's University, Kingston, ON K7L 3N6, Canada

[34] Department of Physics & Astronomy, University of Nevada, Las Vegas, NV, 89154, USA

[35] Nevada Center for Astrophysics, University of Nevada, Las Vegas, NV 89154, USA

[36] Dept. of Physics and Astronomy, University of Kansas, Lawrence, KS 66045, USA

[37] Centre for Cosmology, Particle Physics and Phenomenology - CP3, Université catholique de Louvain, Louvain-la-Neuve, Belgium

[38] Department of Physics, Mercer University, Macon, GA 31207-0001, USA

[39] Dept. of Astronomy, University of Wisconsin–Madison, Madison, WI 53706, USA

[40] Dept. of Physics and Wisconsin IceCube Particle Astrophysics Center, University of Wisconsin–Madison, Madison, WI 53706, USA

[41] Institute of Physics, University of Mainz, Staudinger Weg 7, D-55099 Mainz, Germany

[42] Department of Physics, Marquette University, Milwaukee, WI, 53201, USA

[43] Institut für Kernphysik, Westfälische Wilhelms-Universität Münster, D-48149 Münster, Germany

[44] Bartol Research Institute and Dept. of Physics and Astronomy, University of Delaware, Newark, DE 19716, USA

[45] Dept. of Physics, Yale University, New Haven, CT 06520, USA

[46] Columbia Astrophysics and Nevis Laboratories, Columbia University, New York, NY 10027, USA

[47] Dept. of Physics, University of Oxford, Parks Road, Oxford OX1 3PU, United Kingdom

[48] Dipartimento di Fisica e Astronomia Galileo Galilei, Università Degli Studi di Padova, 35122 Padova PD, Italy

[49] Dept. of Physics, Drexel University, 3141 Chestnut Street, Philadelphia, PA 19104, USA

[50] Physics Department, South Dakota School of Mines and Technology, Rapid City, SD 57701, USA

[51] Dept. of Physics, University of Wisconsin, River Falls, WI 54022, USA

[52] Dept. of Physics and Astronomy, University of Rochester, Rochester, NY 14627, USA

[53] Department of Physics and Astronomy, University of Utah, Salt Lake City, UT 84112, USA

[54] Oskar Klein Centre and Dept. of Physics, Stockholm University, SE-10691 Stockholm, Sweden

[55] Dept. of Physics and Astronomy, Stony Brook University, Stony Brook, NY 11794-3800, USA

[56] Dept. of Physics, Sungkyunkwan University, Suwon 16419, Korea

[57] Institute of Physics, Academia Sinica, Taipei, 11529, Taiwan

[58] Dept. of Physics and Astronomy, University of Alabama, Tuscaloosa, AL 35487, USA

[59] Dept. of Astronomy and Astrophysics, Pennsylvania State University, University Park, PA 16802, USA

[60] Dept. of Physics, Pennsylvania State University, University Park, PA 16802, USA

[61] Dept. of Physics and Astronomy, Uppsala University, Box 516, S-75120 Uppsala, Sweden

[62] Dept. of Physics, University of Wuppertal, D-42119 Wuppertal, Germany

[63] Deutsches Elektronen-Synchrotron DESY, Platanenallee 6, 15738 Zeuthen, Germany

[64] Institute of Physics, Sachivalaya Marg, Sainik School Post, Bhubaneswar 751005, India

[65] Department of Space, Earth and Environment, Chalmers University of Technology, 412 96 Gothenburg, Sweden

[66] Earthquake Research Institute, University of Tokyo, Bunkyo, Tokyo 113-0032, Japan

Acknowledgements